

# Role of Substitution at Terminal Nitrogen of 2-Oxo-1,2-dihydroquinoline-3-Carbaldehyde Thiosemicarbazones on the Coordination Behavior and Structure and Biological Properties of Their Palladium(II) Complexes

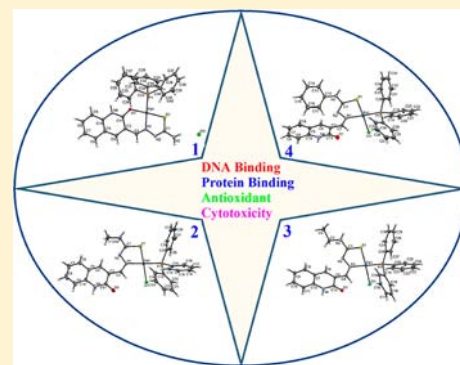
Eswaran Ramachandran,<sup>†</sup> Duraisamy Senthil Raja,<sup>†</sup> Nigam. P. Rath,<sup>‡</sup> and Karuppanan Natarajan<sup>\*†</sup>

<sup>†</sup>Department of Chemistry, Bharathiar University, Coimbatore 641046 India

<sup>‡</sup>Department of Chemistry and Biochemistry and Centre for Nano science, University of Missouri, St. Louis, Missouri 63121, United States

## Supporting Information

**ABSTRACT:** A series of four new palladium(II) complexes of 2-oxo-1,2-dihydroquinoline-3-carbaldehyde thiosemicarbazones with triphenylphosphine as coligand have been synthesized and characterized by the aid of various spectral techniques. The single-crystal X-ray diffraction studies revealed that the unsubstituted thiosemicarbazone ligand acted as monobasic tridentate (ONS<sup>-</sup>) in the cationic [Pd(H-Qtsc-H)(PPh<sub>3</sub>)<sub>3</sub>]Cl complex, whereas the monosubstituted thiosemicarbazone ligands acted as monobasic bidentate (NS<sup>-</sup>) in their respective complexes, [PdCl(H-Qtsc-R)(PPh<sub>3</sub>)<sub>2</sub>] (R = Me (2), Et (3), Ph (4)). To ascertain the potentials of the above Pd(II) complexes toward biomolecular interactions, additional experiments involving interaction with calf thymus DNA and bovine serum albumin were carried out. Moreover, all the palladium(II) complexes have been screened for their radical scavenging activity toward DPPH, O<sub>2</sub><sup>-</sup>, OH, and NO radicals. The efficiency of the complexes in arresting the growth of human cervical cancer cells (HeLa), human laryngeal epithelial carcinoma cells (HEp-2), human liver carcinoma cells (Hep G2), and human skin cancer cells (A431) has also been studied along with the cell viability test against the noncancerous NIH 3T3 mouse embryonic fibroblasts cell lines under in vitro conditions. All the in vitro pharmacological evaluation results clearly revealed the relationship between the structure and the activity of the new Pd(II) complexes.



## INTRODUCTION

Synthesis of new metal complexes with structural design and properties analogous to anticancer agents is one of the most productive areas of coordination chemistry. The fact that DNA and protein biomolecules are electron-rich and metal ions electron-deficient compels one to believe to have strong interactions between metal ions and biomolecules. Therefore, the study of the binding properties of metal complexes with DNA and protein is of great significance for the design of new drugs and their application.<sup>1</sup>

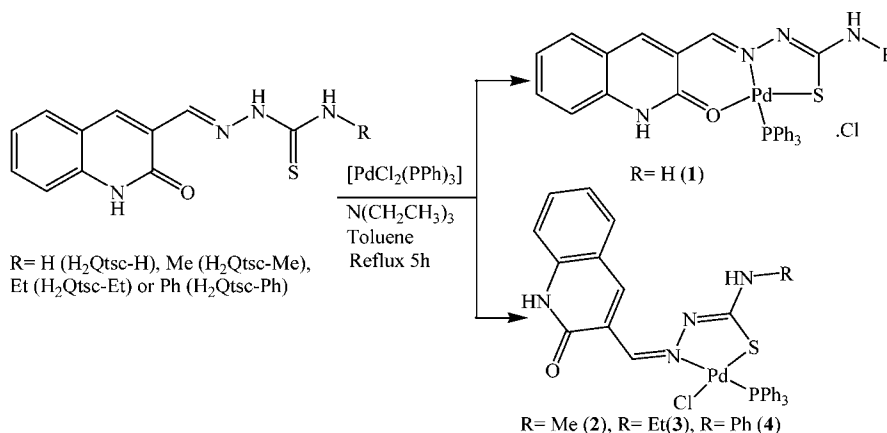
Nowadays, cancer is one of the most important human health concerns in the world, which claims numerous deaths each year and is on the increase worldwide. A majority of drugs used for the treatment of cancer today are not “cancer cell specific” and are potently toxic against normal cells also. This has opened up a new and active area of research in bioinorganic medicinal chemistry. In this regard, cisplatin, carboplatin, and oxaliplatin are well-known metal-based drugs and are widely used to treat solid tumors. However, they have some limitations due to resistance over a period of time and severe side effects in causing nausea and the failure of kidney and liver, which are typical of heavy metal toxicity.<sup>2–5</sup> Hence, attempts are being made to replace this drug with more-efficient, less toxic, and

target-specific noncovalent DNA binding anticancer drugs. On the basis of the structural analogy and thermodynamic similarities with platinum(II) complexes,<sup>6,7</sup> a number of palladium(II) complexes have been reported with their potential antitumor properties.<sup>8–14</sup> On the other hand, nitrogen heterocyclic thiosemicarbazones are proved to be versatile ligands due to their variable coordination behavior and promising biological properties.<sup>15–17</sup> In this area, our group has been actively engaged in the study on the variable coordination behaviors of thiosemicarbazones,<sup>18–27</sup> and on the biological properties of the resulting complexes. Encouraged by our previous results of copper complexes of 2-oxo-1,2-dihydroquinoline-3-carbaldehyde 4*N*-substituted thiosemicarbazones in protein binding, antioxidation, and in vitro cytotoxicity,<sup>22</sup> we choose the same ligand series to study their coordination behavior with Pd(II) and to study the biological applications of the resulting palladium(II) complexes. Herein, we describe the synthesis, structure, DNA and protein binding, antioxidative, and in vitro cytotoxicity studies of mononuclear palladium complexes of 2-oxo-1,2-dihydroquinoline-3-carbalde-

Received: October 16, 2012

Published: January 16, 2013

Scheme 1. Synthetic Route of the New Palladium(II) Complexes



hyde 4*N*-substituted thiosemicarbazones. The crystal structures of all the new palladium(II) complexes have been determined by X-ray crystallography. The synthetic routes of the palladium complexes are shown in Scheme 1.

## EXPERIMENTAL SECTION

**Materials and Methods.** All the reagents used were of analytical or chemically pure grade. Solvents were purified and dried according to standard procedures.<sup>28</sup> Doubly distilled water was used to prepare buffers. Ethidium bromide (EB), bovine serum albumin (BSA), calf thymus DNA (CT-DNA), and 3-(4,5-dimethylthiazol-2-yl)-2,5-diphenyltetrazolium bromide (MTT) were purchased from Sigma-Aldrich and used as received. The ligands and the starting complex, [PdCl<sub>2</sub>(PPh<sub>3</sub>)<sub>2</sub>] were prepared by literature methods.<sup>22,29</sup> Elemental analyses (C, H, N, S) were performed on a Vario EL III Elemental analyzer instrument. Infrared spectra of the ligand and the metal complexes were recorded in the range of 4000–400 cm<sup>-1</sup> using a Nicolet Avatar model FT-IR spectrophotometer from KBr discs. The electronic spectra of the complexes were recorded with a Jasco V-630 spectrophotometer using 5% DMSO in buffer as the solvent. Emission spectra were measured using a Jasco FP 6600 spectrofluorometer. <sup>1</sup>H and <sup>31</sup>P NMR spectra were recorded on a Bruker Avance-3 spectrometer at 400 MHz. The melting points were recorded with a Lab India melting point apparatus.

**Synthesis of Complexes.** [Pd(HQQtsc-H)(PPh<sub>3</sub>)Cl] (1). To a solution of [PdCl<sub>2</sub>(PPh<sub>3</sub>)<sub>2</sub>] (0.100 g, 0.143 mmol) in toluene (20 cm<sup>3</sup>) were added the ligand, H<sub>2</sub>Qtsc-H (0.035 g, 0.143 mmol), and two drops of triethylamine. The mixture was refluxed for 5 h during which period an orange colored precipitate was formed. The reaction mixture was then cooled to room temperature, and the solid compound was filtered. It was washed with toluene and dried under vacuum. Yield: 81%, mp: 244–246 °C. Elemental analysis calculated for C<sub>29</sub>H<sub>24</sub>ClN<sub>4</sub>OPPdS (%): C, 53.63; H, 3.72; N, 8.63; S, 4.97. Found (%): C, 53.49; H, 3.66; N, 8.71; S, 4.76. IR (KBr disks, cm<sup>-1</sup>): 3458(m) ν(NH); 3155(m) ν(NH<sub>2</sub>); 1627 ν(C=O); 1588, 1548 (s) ν(C=N) + ν(C=C); 745 (m) ν(C=S); 1435, 1100, 693 (for PPh<sub>3</sub>). UV–vis (5% DMSO in buffer), λ<sub>max</sub> (nm): 325 (intraligand transition); 381 (LMCT s/d); 410 (MLCT). <sup>1</sup>H NMR (CDCl<sub>3</sub>, ppm): 11.65 (s, 1H, N(4)H); 8.84 (s, 1H, C(2)H); 8.51 (s, 2H, N(1)H<sub>2</sub>); 8.01 (s, 1H, C(4)H); 7.52–7.83 (m, 19H, aromatic). <sup>31</sup>P NMR (CDCl<sub>3</sub>, ppm): 23.92 (s).

The single crystals of **1** grown from methanol/DMF were found to be suitable for X-ray diffraction.

[PdCl(HQQtsc-Me)(PPh<sub>3</sub>)] (2). It was prepared using the same procedure as described for **1** by the reaction of [PdCl<sub>2</sub>(PPh<sub>3</sub>)<sub>2</sub>] (0.100 g, 0.143 mmol) with ligand, H<sub>2</sub>Qtsc-Me (0.037 g, 0.143 mmol). A dark orange colored precipitate was formed. The filtered solid compound was then washed with toluene and dried under vacuum. Yield: 78%, mp: 267–269 °C. Elemental analysis calculated for C<sub>30</sub>H<sub>26</sub>ClN<sub>4</sub>OPPdS (%): C, 54.31; H, 3.95; N, 8.44; S, 4.83. Found

(%): C, 54.47; H, 3.82; N, 8.51; S, 4.76. IR (KBr disks, cm<sup>-1</sup>): 3317 (m) ν(NH); 1654 ν(C=O); 1600, 1552 (s) ν(C=N) + ν(C=C); 778 (m) ν(C-S); 1427, 1086, 681 (for PPh<sub>3</sub>). UV–vis (5% DMSO in buffer), λ<sub>max</sub> (nm): 417; 438 (MLCT). <sup>1</sup>H NMR (CDCl<sub>3</sub>, ppm): δ 11.75 (s, 1H, N(4)H); 9.95 (s, 1H, N(3)H); 9.02 (s, 1H, C(2)H); 8.01 (s, 1H, C(4)H); 7.20–7.79 (m, 19H, aromatic); 2.78 (s, 3H, C(12)H). <sup>31</sup>P NMR (CDCl<sub>3</sub>, ppm): 22.99 (s).

The single crystals of **2** grown from methanol/DMF were found to be suitable for X-ray diffraction studies.

[PdCl(HQQtsc-Et)(PPh<sub>3</sub>)] (3). It was prepared as described for **1** by the reaction of [PdCl<sub>2</sub>(PPh<sub>3</sub>)<sub>2</sub>] (0.100 g, 0.143 mmol) with ligand, H<sub>2</sub>Qtsc-Et (0.039 g, 0.143 mmol). Dark orange colored crystals obtained in the reaction mixture itself were found to be suitable for X-ray diffraction. Yield: 74%, mp: 261–263 °C. Elemental analysis calculated for C<sub>31</sub>H<sub>28</sub>ClN<sub>4</sub>OPPdS (%): C, 54.96; H, 4.17; N, 8.27; S, 4.73. Found (%): C, 54.83; H, 4.26; N, 8.41; S, 4.62. IR (KBr disks, cm<sup>-1</sup>): 3316 (m) ν(NH); 1644 (s) ν(C=O); 1589, 1550 (s) ν(C=N) + ν(C=C); 752 (m) ν(C-S); 1433, 1097, 693 (for PPh<sub>3</sub>). UV–vis (5% DMSO in buffer), λ<sub>max</sub> (nm): 417 (LMCT s/d); 441 (MLCT). <sup>1</sup>H NMR (CDCl<sub>3</sub>): δ 11.31 (s, N(4)H); 8.82 (s, 1H, N(3)H); 8.45 (s, 1H, 6(3)H); 8.21 (s, 1H, C(4)H); 7.34–7.77 (m, 19H, aromatic); 3.24 (q, 2H, C(2)H); 1.18 (t, 3H, C(3)H). <sup>31</sup>P NMR (CDCl<sub>3</sub>, ppm): 30.18 (s).

[PdCl(HQQtsc-Ph)(PPh<sub>3</sub>)] (4). It was prepared as described for **1** by the reaction of [PdCl<sub>2</sub>(PPh<sub>3</sub>)<sub>2</sub>] (0.100 g, 0.143 mmol) with ligand, H<sub>2</sub>Qtsc-Ph (0.046 g, 0.143 mmol). A dark orange colored precipitate formed was filtered. Yield: 79%, mp: 276–278 °C. Elemental analysis calculated for C<sub>35</sub>H<sub>28</sub>ClN<sub>4</sub>OPPdS (%): C, 57.94; H, 3.89; N, 7.72; S, 4.42. Found (%): C, 57.79; H, 3.96; N, 7.67; S, 4.52. IR (KBr disks, cm<sup>-1</sup>): 3261 (m) ν(NH); 1660 ν(C=O); 1593, 1549 (s) ν(C=N) + ν(C=C); 745 (m) ν(C-S); 1433, 1102, 653 (for PPh<sub>3</sub>). UV–vis (5% DMSO in buffer), λ<sub>max</sub> (nm): 394 (LMCT s/d); 427 (MLCT). <sup>1</sup>H NMR (CDCl<sub>3</sub>): δ 11.16 (s, N(4)H); δ 8.82 (s, 1H, N(3)H); 8.37 (s, 1H, C(2)H); 8.05 (s, 1H, C(4)H); 7.22–7.78 (m, 24H, aromatic); 3.81 (s, 3H, C(11)H). <sup>31</sup>P NMR (CDCl<sub>3</sub>, ppm): 29.77 (s).

The crystals of **4** grown from methanol/DMF solution were found to be suitable for X-ray diffraction.

**Single-Crystal X-ray Diffraction Studies.** Suitable crystals of **1**–**4** with approximate dimensions of 0.30 × 0.27 × 0.22, 0.42 × 0.19 × 0.07, 0.27 × 0.26 × 0.14, and 0.29 × 0.17 × 0.11 mm<sup>3</sup> were mounted on a Mitgen cryoloop in a random orientation. Preliminary examination and the data collection were performed by using a Bruker Kappa Apex-II or Bruker SMART Charge Coupled Device (CCD) Detector system single-crystal X-ray diffractometer equipped with an Oxford Cryostream LT device. All the data were collected using graphite monochromated Mo Kα radiation (λ = 0.71073 Å) from a fine focus sealed tube X-ray source. Preliminary unit cell constants were determined with a set of 36 narrow frame scans. Typical data sets consist of combinations of φ and θ scan frames with a typical scan width of 0.5° and a counting time of 15–30 s/frame at a crystal-to-detector distance of ~3.5 to 5.0 cm. The collected frames

Table 1. Experimental Data for Crystallographic Analyses

	complex 1	complex 2	complex 3	complex 4
CCDC number	905160	905161	905162	905163
empirical formula	C <sub>30.50</sub> H <sub>31</sub> ClN <sub>4</sub> O <sub>3</sub> PPdS	C <sub>33</sub> H <sub>33</sub> ClN <sub>5</sub> O <sub>2</sub> PPdS	C <sub>31</sub> H <sub>28</sub> ClN <sub>4</sub> OPPdS	C <sub>38</sub> H <sub>35</sub> ClN <sub>5</sub> O <sub>2</sub> PPdS
formula weight	706.47	736.52	677.45	798.59
cryst syst	triclinic	triclinic	triclinic	monoclinic
space group	$P\bar{1}$	$P\bar{1}$	$P\bar{1}$	$P2_1/n$
<i>a</i> (Å)	11.3651(11)	9.8780(6)	13.3608(8)	9.4819(6)
<i>b</i> (Å)	12.5237(12)	12.6222(9)	15.2074(9)	15.8125(10)
<i>c</i> (Å)	23.108(2)	14.4435(9)	15.5413(9)	23.7818(16)
$\alpha$ (deg)	91.867(4)	77.362(4)	107.780(3)	
$\beta$ (deg)	93.783(5)	80.739(3)	108.265(2)	100.169(4)
$\gamma$ (deg)	111.151(4)	69.568(2)	90.049(3)	
<i>Z</i>	4	2	4	4
density (calcd), Mg/m <sup>3</sup>	1.536	1.492	1.585	1.511
<i>F</i> (000)	1440	752	1376	1632
$\theta$ for data collection (deg)	1.75–28.77	1.75–38.53	1.61–38.27	2.16–36.95
goodness of fit on <i>F</i> <sup>2</sup>	1.063	1.010	1.026	1.034

were integrated using an orientation matrix determined from the narrow frame scans. Apex II and SAINT software packages<sup>30</sup> were used for data collection and data integration.

Analysis of the integrated data did not show any decay. Final cell constants were determined by global refinement of reflections from the complete data set. Data were corrected for systematic errors using SADABS<sup>30</sup> based on the Laue symmetry using equivalent reflections. The structures were solved by direct methods and refined successfully. Structure solution and refinement were carried out using the SHELXTL-PLUS software package.<sup>31</sup> Full-matrix least-squares refinement was carried out by minimizing  $\sum w(F_o^2 - F_c^2)^2$ . For all the complexes, the non-hydrogen atoms were refined anisotropically to convergence. Typically, H atoms were added at the calculated positions in the final refinement cycles. All other hydrogen atoms were treated using the appropriate riding model. Complex 1 has one molecule of water and three molecules of MeOH (two were disordered) in the lattice. Of the two chloride ions, one is disordered and refined in two positions (59:41%). Disordered atoms were refined with restraints as needed. Complex 2 has a molecule of disordered DMF in the lattice, and the disordered solvent atoms were refined with geometrical and displacement parameter restraints. Crystal data and details of the structure refinement for complexes 1–4 are listed in Table 1.

**DNA Binding and Protein Binding Studies.** All of the experiments involving the binding of compounds with CT-DNA and with BSA (protein) were carried out as described earlier.<sup>43</sup>

**Antioxidant Assays.** The hydroxyl radical scavenging activity of the complexes has been investigated using the Nash method.<sup>32</sup> For the hydroxyl radical scavenging studies, in vitro hydroxyl radicals were generated with the Fe<sup>3+</sup>/ascorbic acid system. The detection of hydroxyl radicals was carried out by measuring the amount of formaldehyde formed from the oxidation of DMSO.<sup>33</sup> The formaldehyde produced was detected spectrophotometrically at 412 nm. A mixture of 1.0 mL of an iron–EDTA solution (0.13% ferrous ammonium sulfate and 0.26% EDTA), 0.5 mL of EDTA solution (0.018%), and 1.0 mL of DMSO (0.85% DMSO (v/v) in 0.1 M phosphate buffer, pH 7.4) was sequentially added in the test tubes containing test solutions. The reaction was initiated by adding 0.5 mL of ascorbic acid (0.22%) and incubated at 80–90 °C for 15 min in a water bath. After incubation, the reaction was terminated by the addition of 1.0 mL of ice-cold trichloroacetic acid (17.5% w/v). Subsequently, 3.0 mL of Nash reagent (mixture of ammonium acetate, glacial acetic acid, and acetyl acetone) was added to each tube and left at room temperature for 15 min. The intensity of the color formed was measured spectrophotometrically at 412 nm against a reagent blank.

The assay of nitric oxide scavenging activity was based on the method<sup>34</sup> where sodium nitroprusside in aqueous solution at physiological pH spontaneously generates nitric oxide, which interacts

with oxygen to produce nitrite ions that can be estimated using the Greiss reagent. Scavengers of nitric oxide compete with oxygen, leading to reduced production of nitrite ions. For the experiment, sodium nitroprusside (10 mM) in phosphate buffered saline was mixed with a fixed concentration of the compound and incubated at room temperature for 150 min. After the incubation period, 0.5 mL of the Griess reagent containing 1% sulfanilamide, 2% H<sub>3</sub>PO<sub>4</sub>, and 0.1% *N*-(1-naphthyl)ethylenediamine dihydrochloride was added. The absorbance of the chromophore formed was measured at 546 nm.

The 2,2-Diphenyl-1-picrylhydrazyl (DPPH) radical scavenging activity of the compounds was measured according to the method of Blois.<sup>35</sup> The DPPH radical is a stable free radical having a  $\lambda_{max}$  at 517 nm. A fixed concentration of the experimental compound was added to a solution of DPPH in methanol (125  $\mu$ M, 2 mL), and the final volume was made up to 4 mL with double distilled water. The solution was incubated at 37 °C for 30 min in the dark. The decrease in absorbance of DPPH was measured at 517 nm.

The superoxide anion radical scavenging assay was based on the capacity of the compounds to inhibit formazan formation by scavenging the superoxide radicals generated in a riboflavin–light–nitroblue tetrazolium system.<sup>36</sup> Each 3 mL of reaction mixture contained 50 mM sodium phosphate buffer (pH 7.6), 20  $\mu$ g of riboflavin, 12 mM EDTA, 0.1 mg of nitroblue tetrazolium, and 1 mL of test solution (20–100  $\mu$ g/mL). The reaction was started by illuminating the reaction mixture with different concentrations of the compounds for 90 s. Immediately after illumination, the absorbance was measured at 590 nm. The entire reaction assembly was enclosed in a box lined with aluminum foil. Identical tubes with the reaction mixture kept in the dark served as blanks.

For the above four assays, all of the tests were run in triplicate, and various concentrations of the compounds were used to fix a concentration at which the compounds showed in and around 50% of activity. In addition, the percentage of activity was calculated using the formula, % of suppression ratio =  $[(A_0 - A_C)/A_0] \times 100$ . *A*<sub>0</sub> and *A*<sub>C</sub> are the absorbance in the absence and presence of the tested compounds, respectively. The 50% activity (*IC*<sub>50</sub>) can be calculated using the percentage of activity.

#### In Vitro Anticancer Activity Evaluation by MTT Assays.

Cytotoxicity studies of the free ligands, [PdCl<sub>2</sub>(PPh<sub>3</sub>)<sub>2</sub>], and new complexes along with cisplatin were carried out on human cervical cancer cells (HeLa), human liver carcinoma cells (Hep G2), human skin cancer cells (A431), human laryngeal epithelial carcinoma cells (Hep-2), and NIH 3T3 normal cells (mouse embryonic fibroblasts), which were obtained from the National Centre for Cell Science, Pune, India. Cell viability was carried out using the MTT assay method.<sup>37</sup> The HeLa, A431, Hep G2, and Hep-2 cancer cells were grown in Eagles minimum essential medium containing 10% fetal bovine serum (FBS), whereas NIH 3T3 fibroblasts were grown in Dulbecco

modified Eagles medium (DMEM) containing 10% FBS. For the screening experiments, the cells were seeded into 96-well plates in 100  $\mu\text{L}$  of the respective medium containing 10% FBS, at a plating density of 10 000 cells/well, and incubated at 37  $^{\circ}\text{C}$ , under conditions of 5%  $\text{CO}_2$ , 95% air, and 100% relative humidity for 24 h prior to the addition of compounds. The compounds were dissolved in DMSO and diluted in the respective medium containing 1% FBS. After 24 h, the medium was replaced with the respective medium with 1% FBS containing the complexes at various concentrations and incubated at 37  $^{\circ}\text{C}$  under conditions of 5%  $\text{CO}_2$ , 95% air, and 100% relative humidity for 48 h. Triplication was maintained, and the medium not containing the complexes served as the control. After 48 h, 10  $\mu\text{L}$  of MTT (5 mg/mL) in phosphate buffered saline (PBS) was added to each well and incubated at 37  $^{\circ}\text{C}$  for 4 h. The medium with MTT was then flicked off, and the formed formazan crystals were dissolved in 100  $\mu\text{L}$  of DMSO. The absorbance was then measured at 570 nm using a microplate reader. The percentage of cell inhibition was determined using the formula, % inhibition = [mean OD of untreated cells (control)/mean OD of treated cells (control)]  $\times$  100. From the plot of percentage of cell inhibition versus concentration, the  $\text{IC}_{50}$  value was calculated.

## RESULTS AND DISCUSSION

**Synthesis and Characterization.** A series of four new palladium(II) complexes of 2-oxo-1,2-dihydroquinoline-3-carbaldehyde 4*N*-substituted thiosemicarbazones, {[Pd(HQts-c-H)PPh<sub>3</sub>]<sub>2</sub>Cl} (1), [PdCl(HQts-c-Me)PPh<sub>3</sub>] (2), [PdCl(HQts-c-Et)PPh<sub>3</sub>] (3), [PdCl(HQts-c-Ph)PPh<sub>3</sub>] (4)}, have been obtained by the direct reaction of the [PdCl<sub>2</sub>(PPh<sub>3</sub>)<sub>2</sub>] with the corresponding ligands. It has been observed that the unsubstituted ligand coordinated as monobasic tridentate (in 1), whereas all other ligands coordinated as monobasic bidentate (in 2–4). All the new palladium complexes were characterized by elemental analysis, IR, UV–vis, <sup>1</sup>H NMR, and <sup>31</sup>P NMR spectroscopy, and the significant data are given in the Experimental Section. The IR peak shift in  $\nu(\text{C}=\text{N})$ ,  $\nu(\text{C}=\text{O})$ , and  $\nu(\text{C}=\text{S})$  of the ligands in the complexes gave evidence for the coordination of the ligand to palladium ion. Though the  $\nu(\text{C}=\text{O})$  IR peak was slightly shifted for 1, there were no significant changes in  $\nu(\text{C}=\text{O})$  for complexes 2–4 when compared to that of the free ligands, indicating that the oxo group oxygen was not coordinated to the palladium ion. In the <sup>1</sup>H NMR spectra of the new complexes, the absence of the signal for N(2)H indicated that sulfur coordinated to the palladium ion in complexes 1–4 in the thiolate form, which has also been confirmed by single-crystal X-ray diffraction studies. The presence of the peak for N(4)H in all the complexes clearly indicated that the oxygen remained as oxo and not coordinated with palladium ion; but in complex 1, it coordinated as the neutral form with the palladium atom. These above observations have been confirmed by X-ray single-crystal structure analysis.

**Crystal Structure of Complexes 1–4.** The ORTEP view of complex 1 along with the atomic numbering scheme is given in Figure 1. The crystallographic data showed that complex 1 is crystallized in a triclinic crystal system with the space group  $P\bar{1}$  and two asymmetric units are present. The Pd(II) ion adopts a distorted square-planar geometry with the binding of the ligand as monobasic tridentate (ONS donor), and the fourth site is occupied by a triphenylphosphine ligand. The charge on the complex is neutralized by one chloride ion that is present in the lattice. The trans angles of O(1)–Pd(1)–S(1), 177.15(4) $^{\circ}$ , and N(1)–Pd(1)–P(1), 175.19(5) $^{\circ}$ , indicated a slight deviation from the expected linear trans geometry, suggesting distortion in the square-planar coordination geometry. The dihedral angle

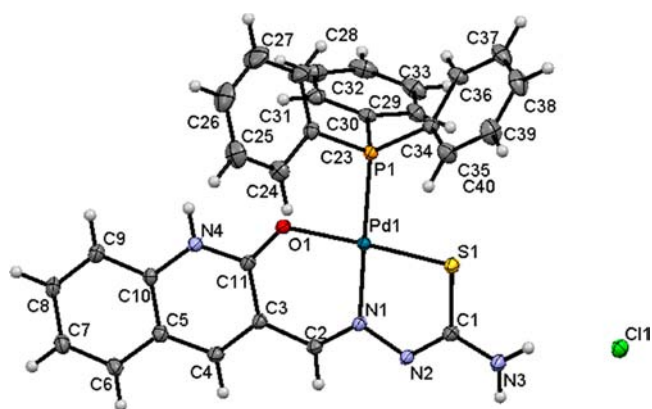


**Figure 1.** ORTEP view of complex 1. The methanol and water molecules have been omitted for clarity.

between the mean planes of the five-membered chelation ring and the six-membered one is 6.02 $^{\circ}$ . An analysis of the molecular packing diagram of complex 1 revealed that the intermolecular interaction makes a pseudo binuclear structure (Figure S1, Supporting Information).

The molecular structures of complexes 2–4 together with the atomic numbering scheme are shown in Figures 2, 3, and 4.

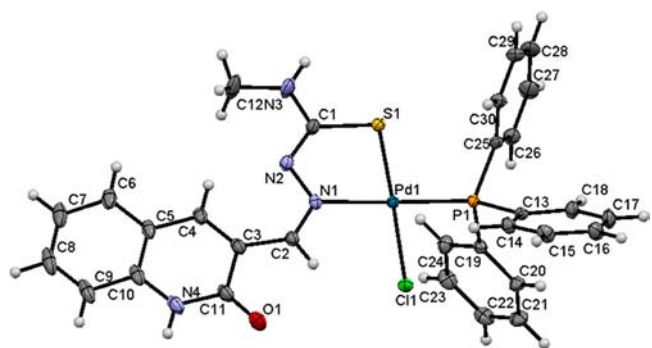


**Figure 2.** ORTEP view of complex 3. The solvated DMF molecule has been omitted for clarity.

The single-crystal X-ray studies revealed that complexes 2 and 3 are crystallized in a triclinic system with the space group  $P\bar{1}$ , whereas complex 4 crystallized in a monoclinic system with the space group  $P2_1/n$ . In complexes 2–4, the coordination geometry around Pd(II) is a distorted square-planar, the palladium atom being bonded to uninegative bidentate NS

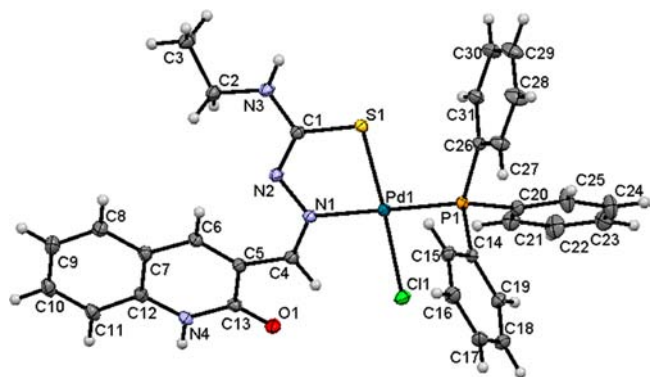


**Figure 3.** ORTEP view of complex 3.

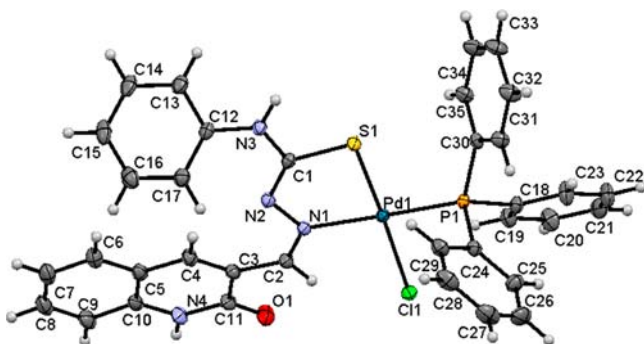


**Figure 4.** ORTEP view of complex 4. The solvated DMF molecule has been omitted for clarity.

donor ligand molecules in such a way that a five-membered ring is formed. The remaining sites are occupied by chloride and triphenylphosphine. The trans angles are S(1)–Pd(1)–Cl(1), 175.461(12)°, and N(1)–Pd(1)–P(1), 172.94(3)° (for 2), S(1)–Pd(1)–Cl(1), 176.242(12)°, and N(1)–Pd(1)–P(1), 176.65(3)° (for 3), and of complex 4 are S(1)–Pd(1)–Cl(1), 177.41(12)°, and N(1)–Pd(1)–P(1), 169.96(3)°, which showed a deviation from the expected linear trans geometry, suggesting distortion in the square-planar coordination geometry. The molecular packing diagram analysis of the complexes suggested that the stabilization of the lattice was effected by several hydrogen bonds. In complexes 2–4, the pyridine hydrogen atom is involved in intermolecular hydrogen bonding with the oxygen atom of a second molecule, N(4)–H(4)⋯O(1) and O(1)⋯N(4)–H(4) (Figures S2–S4, Supporting Information). These intermolecular hydrogen bonds give a pseudo binuclear structure for all the complexes. The selected bond lengths and bond angles are summarized in Table 2, and they agree very well with those that are reported for other palladium(II) complexes.<sup>24,26</sup>

**DNA Binding Studies.** DNA binding is a significant footstep for chemical nuclease activity of the metal complexes. Therefore, before evaluating the potentials of antitumor activities of the new complexes, the interaction between DNA and the new synthesized complexes was examined. The mode and tendency for the binding of complexes 1–4 to CT-DNA were studied with different methods.

**Electronic Absorption Titration.** Electronic absorption spectroscopy is one of the most common techniques used for investigating the mode of binding between the metal complexes and DNA.<sup>38</sup> In general, the metal complexes binding to DNA through intercalation results in hypochromism with or without a small red or blue shift, since the intercalative mode involves in a strong stacking interaction between the planar aromatic chromophore and the base pairs of DNA.<sup>21,39</sup> The representative absorption spectra of the complexes in the absence and presence of CT-DNA are shown in Figure 5. It is seen from the spectra that, as the concentration of DNA is gradually increased, significant changes were observed in intensity of the intraligand  $\pi \rightarrow \pi^*$  absorption bands (273–325 nm) and metal-to-ligand ( $\pi \rightarrow \pi^*$ ) charge-transfer (MLCT) bands (381–427 nm) of complexes 1–4, which showed increasing hypochromism with a small red shift (Table 3). These results indicated that all the new palladium complexes bind to the DNA helix via intercalation. The above observations were comparable to those reported earlier for various metallointercalators.<sup>26</sup> However, complex 1 showed more hypochromicity when compared to that of complexes 2–4, indicating that the binding strength of complex 1 is much stronger than that of the other three complexes. To further compare the binding strength of the palladium complexes, their intrinsic binding constants ( $K_b$ ) were determined from the following equation<sup>40</sup>

$$[\text{DNA}]/(\epsilon_a - \epsilon_f) = [\text{DNA}]/(\epsilon_b - \epsilon_f) + 1/K_b(\epsilon_b - \epsilon_f)$$

where [DNA] is the concentration of DNA in the base pairs,  $\epsilon_a$  is the apparent absorption coefficient corresponding to  $A_{\text{obs}}/[\text{compound}]$ ,  $\epsilon_f$  is the extinction coefficient of the free compound, and  $\epsilon_b$  is the extinction coefficient of the compound when fully bound to DNA.

From the plot of  $[\text{DNA}]/(\epsilon_a - \epsilon_f)$  versus [DNA] (Figure 6), the intrinsic binding constant  $K_b$  was calculated from the ratio of the slope and the intercept. The intrinsic binding constant ( $K_b$ ) values of complexes 1–4 are given in Table 3. The experimental values of  $K_b$  clearly indicated that complexes 1–4 bind to DNA via the intercalative mode. From the values obtained, it is inferred that the cationic nature of complex 1 enhances the binding ability with CT-DNA when compared to the rest of the complexes. The overall binding affinity of the complexes is in the order 2 < 3 < 4 < 1. Though it has been

**Table 2.** Selected Bond Lengths [Å] and Angles [deg]

	complex 1	complex 2	complex 3	complex 4
Pd(1)–N(1)	2.0355(17)	2.0921(9)	2.0850(11)	2.0993(10)
Pd(1)–O(1)	2.0594(15)			
Pd(1)–S(1)	2.2291(6)	2.2430(3)	2.2563(3)	2.2377(3)
Pd(1)–P(1)	2.26604(6)	2.2447(3)	2.2648(3)	2.2590(3)
Pd(1)–Cl(1)		2.3350(3)	2.3287(3)	2.3423(3)
N(1)–Pd(1)–O(1)	92.04(6)			
N(1)–Pd(1)–Cl(1)		95.27(3)	92.85(3)	95.06(3)
N(1)–Pd(1)–S(1)	85.35(5)	83.91(3)	83.44(3)	82.62(3)
O(1)–Pd(1)–S(1)	177.15(4)			
S(1)–Pd(1)–Cl(1)		175.461(12)	176.242(12)	177.406(12)
N(1)–Pd(1)–P(1)	175.19(5)	172.94(3)	176.65(3)	169.96(3)
O(1)–Pd(1)–P(1)	87.09(4)			
P(1)–Pd(1)–Cl(1)		87.953(11)	88.067(12)	90.297(12)
S(1)–Pd(1)–P(1)	95.41(2)	92.375(11)	95.668(12)	91.835(12)

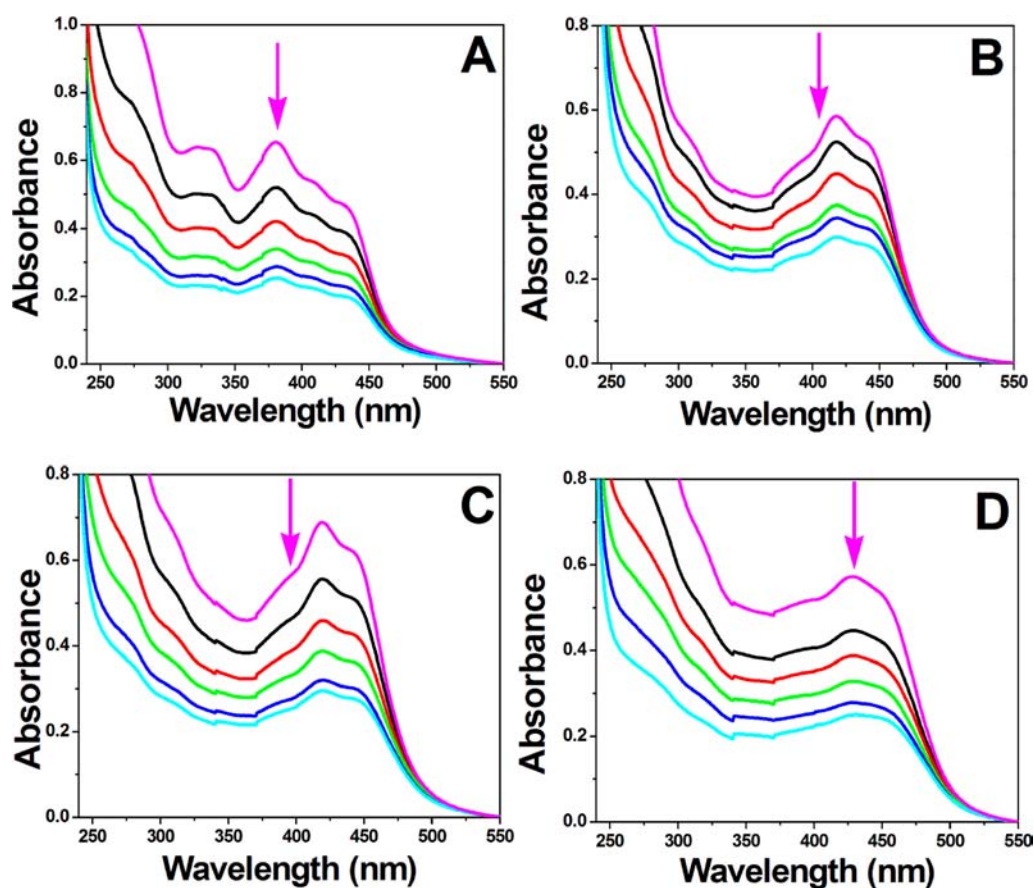


**Figure 5.** Electronic spectra of complexes 1 (A), 2 (B), 3 (C), and 4 (D) in Tris-HCl buffer upon addition of CT-DNA. [Complex] = 25  $\mu\text{M}$ , [DNA] = 0–50  $\mu\text{M}$ . Arrow shows that the absorption intensities decrease upon increasing DNA concentration.

**Table 3.** Absorption Spectral Properties of the Palladium(II) Complexes Bound to CT DNA

complexes	$\lambda_{\text{max}}$ (nm)	change in absorbance	$\Delta\varepsilon$ (%)	red shift (nm)	$K_b$ ( $\text{M}^{-1}$ )
1	380	hypochromism	61	1	$2.64 \times 10^4$
2	418	hypochromism	48		$6.33 \times 10^3$
3	419	hypochromism	57	2	$2.02 \times 10^4$
4	428	hypochromism	56	1	$2.28 \times 10^4$

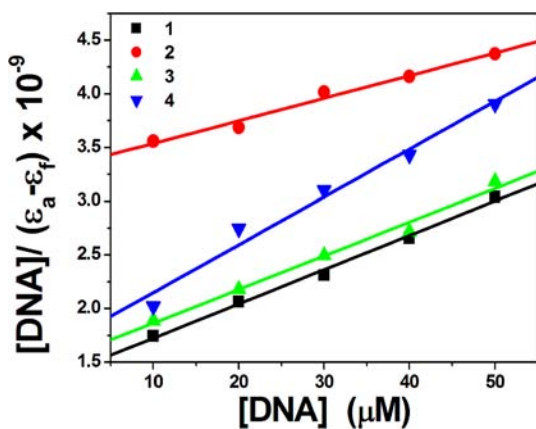


**Figure 6.** Plots of  $[\text{DNA}]/(\varepsilon_a - \varepsilon_f)$  versus  $[\text{DNA}]$  for complexes 1–4 with CT-DNA.

found that complexes 1–4 can bind to DNA by intercalation, the binding mode needs to be proved through further experiments.

**Ethidium Bromide (EB) Displacement Studies.** Ethidium bromide displacement experiments were carried out in order to confirm the binding mode and compare their binding affinities. EB is a planar, cationic dye, and it is widely used as a sensitive fluorescence probe for native DNA. In general, EB emits intense fluorescent light in the presence of DNA due to its strong intercalation between the adjacent DNA base pairs.<sup>41,42</sup> Hence, the EB displacement technique can provide indirect evidence for the DNA binding mode. The displacement technique is based on the decrease of fluorescence resulting from the displacement of EB from a DNA sequence by a quencher, and the quenching is due to the reduction of the number of binding sites on the DNA that is available to the EB. The emission spectra of the DNA–EB system with increasing the concentration of the Pd(II) complexes are shown in Figure 7, and the experimental data are given in Table 4. From the observed decrease in the fluorescence intensity, it has been inferred that the EB molecules are displaced from their DNA binding sites and are replaced by the complexes under investigation.<sup>22</sup> The quenching parameter can be analyzed according to the Stern–Volmer equation

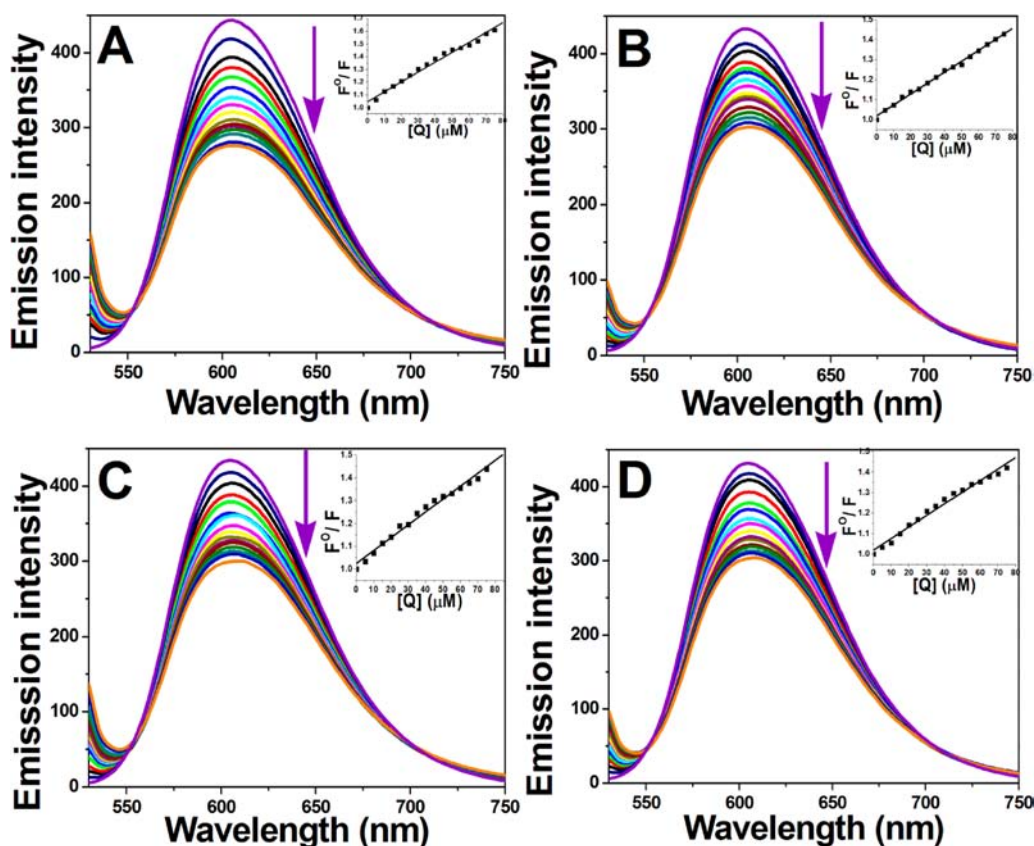


**Figure 7.** Emission spectra of the DNA–EB system,  $\lambda_{\text{exc}} = 515 \text{ nm}$ ,  $\lambda_{\text{emi}} = 530\text{--}750 \text{ nm}$ , in the presence of complexes 1 (A), 2 (B), 3 (C), and 4 (D).  $[\text{DNA}] = 12 \mu\text{M}$ ,  $[\text{Complex}] = 0\text{--}75 \mu\text{M}$ ,  $[\text{EB}] = 12 \mu\text{M}$ . Arrow shows that the emission intensity changes upon increasing complex concentration. Inset: Stern–Volmer plots of the EB–DNA fluorescence titration for complexes 1–4.

**Table 4.** Emission Spectral Properties of the Palladium(II) Complexes Bound to BSA

complexes	$\lambda_{\text{max}}$ (nm)	change in emission	$\Delta\epsilon$ (%)	red shift (nm)	$K_{\text{q}}$ ( $\text{M}^{-1}$ )	$K_{\text{app}}$ ( $\text{M}^{-1}$ )
1	605	hypochromism	37.83	1	$7.78 \times 10^3$	$9.34 \times 10^5$
2	604	hypochromism	30.04	3	$5.43 \times 10^3$	$6.52 \times 10^5$
3	604	hypochromism	30.38	4	$5.65 \times 10^3$	$6.78 \times 10^5$
4	604	hypochromism	29.63	4	$5.64 \times 10^3$	$6.77 \times 10^5$

$$F^0/F = K_{\text{q}}[\text{Q}] + 1$$

where  $F^0$  is the emission intensity in the absence of compound,  $F$  is the emission intensity in the presence of compound,  $K_{\text{q}}$  is the quenching constant, and  $[\text{Q}]$  is the concentration of the compound. The  $K_{\text{q}}$  value is obtained as a slope from the plot of  $F^0/F$  versus  $[\text{Q}]$ . From the Stern–Volmer plot (inset in Figure 7) of  $F^0/F$  versus  $[\text{Q}]$ , the quenching constant ( $K_{\text{q}}$ ) values were obtained from the slope, which are listed in Table 4. Further, the apparent DNA binding constant ( $K_{\text{app}}$ ) values were also calculated using the following equation

$$K_{\text{EB}}[\text{EB}] = K_{\text{app}}[\text{complex}]$$

(where the compound concentration is the value at a 50% reduction in the fluorescence intensity of EB,  $K_{\text{EB}}$  ( $1.0 \times 10^7 \text{ M}^{-1}$ ) is the DNA binding constant of EB,  $[\text{EB}]$  is the concentration of EB =  $12 \mu\text{M}$ ), and they are given in Table 4. From these observed data, it is seen that complex 1 has more binding affinities than the other complexes, which is in agreement with the results observed from the electronic absorption spectra. Moreover, the experimental quenching constants and binding constants of the palladium(II) complexes

suggested that the interaction of complexes 1–4 with DNA should be of intercalation.<sup>24</sup> It is further confirmed that complex (1) having a tricoordinated ligand has a higher binding affinity than the rest of the complexes.

**Protein Binding Studies. Fluorescence Quenching of BSA by Mononuclear Palladium(II) Complexes.** It is well-known that the transport of drugs through the bloodstream is affected via the interaction of drugs with blood plasma proteins, particularly with serum albumin. In general, the binding of drugs to these proteins may lead to either a loss or an enhancement of the biological properties of the original drug. Fluorescence spectra are usually employed to qualitatively analyze the binding of chemical compounds to BSA. The fluorescence of BSA is caused by two intrinsic characteristics of the protein, namely, tryptophan and tyrosine. The intrinsic fluorescence of BSA will provide considerable information on their structure and dynamics and is often utilized in the study of protein folding and association reactions. The binding of BSA with the complexes was studied by fluorescence measurement at room temperature. Various concentrations of complexes 1–4 (0–25  $\mu\text{M}$ ) were added to the solution of BSA (1  $\mu\text{M}$ ), and the fluorescence spectra were recorded in the range of 290–450

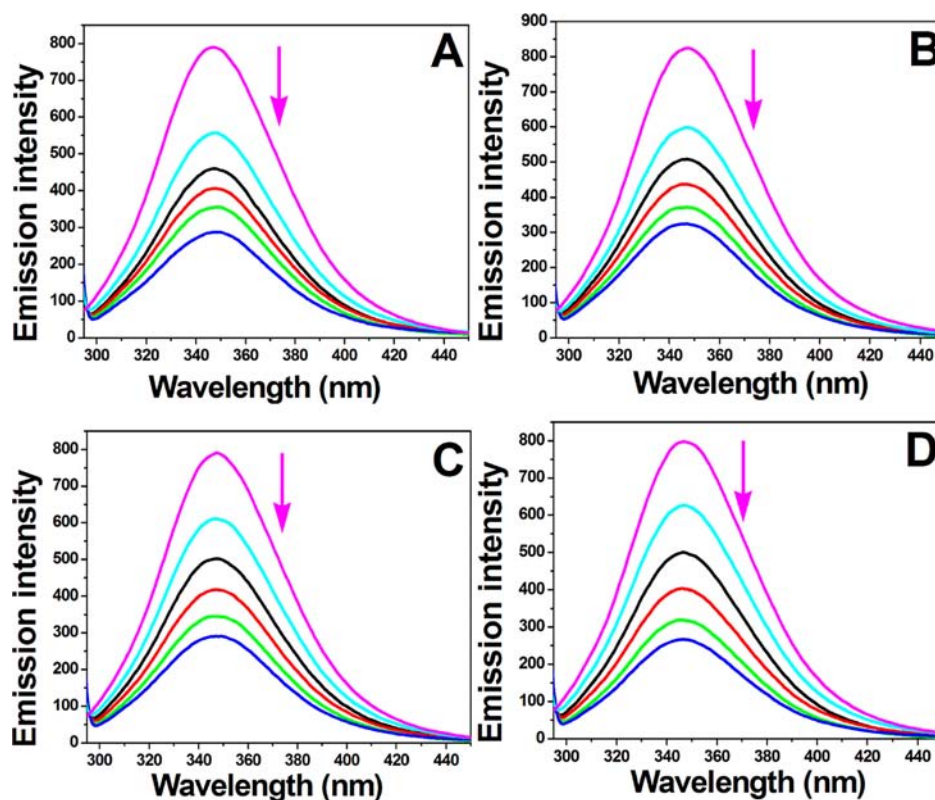


**Figure 8.** Emission spectrum of BSA ( $1 \mu\text{M}$ ;  $\lambda_{\text{exc}} = 280 \text{ nm}$ ;  $\lambda_{\text{emi}} = 346 \text{ nm}$ ) in the presence of increasing amounts of complexes 1 (A), 2 (B), 3 (C), and 4 (D) ( $0$ – $25 \mu\text{M}$ ). Arrow shows that the emission intensity changes upon increasing complex concentration.

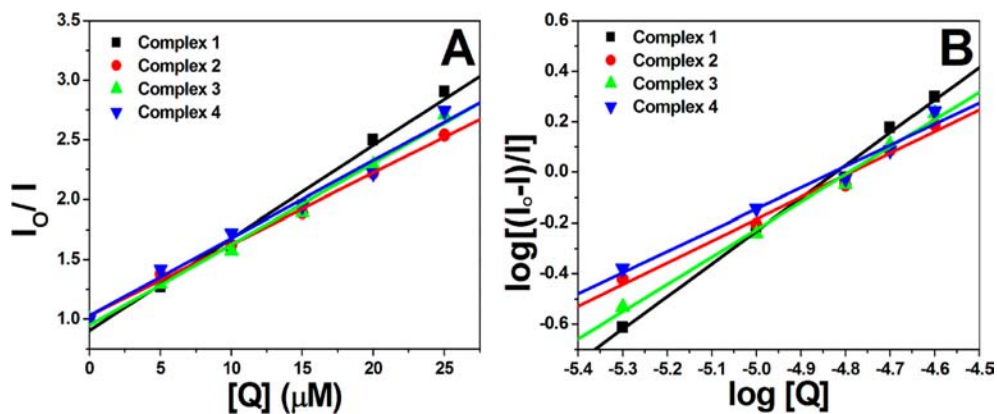


**Figure 9.** Stern–Volmer (A) and Scatchard (B) plot of the BSA fluorescence titration for complexes 1–4.

nm upon excitation at 280 nm. The effects of the complexes on the fluorescence emission spectrum of BSA are given in Figure 8. Upon the addition of the new complexes to the solution of BSA, a significant decrease of the fluorescence intensity of BSA at 346 nm, up to 87.94, 79.45, 85.52 and 87.49%, from the initial fluorescence intensity of BSA, accompanied by a hypsochromic shift of 1–3 nm for complexes 1–4, has been observed respectively. The observed hypsochromicity with blue shift has revealed that all the complexes bind with the BSA protein.<sup>26,38</sup> In addition, fluorescence quenching data were analyzed with the Stern–Volmer equation and Scatchard equation. From the plot of  $I_0/I$  versus  $[Q]$ , the quenching constant ( $K_q$ ) can be calculated (Figure 9A). If it is assumed that the binding of compounds with BSA occurs at equilibrium, the equilibrium binding constant can be analyzed according to the Scatchard equation

$$\log[I_0 - I/I] = \log K_{\text{bin}} + n \log [Q]$$

where  $K_{\text{bin}}$  is the binding constant of the compound with BSA and  $n$  is the number of binding sites. The binding constant ( $K_{\text{bin}}$ ) and the number of binding sites ( $n$ ) have been calculated from the plot of  $\log[(I_0 - I)/I]$  versus  $\log [Q]$  (Figure 9B). The calculated  $K_q$ ,  $K_{\text{bin}}$ , and  $n$  values are listed in Table 5. The calculated value of  $n$  is around 1 for all of the complexes, indicating the existence of just a single binding site in BSA for all of the complexes. However, the results showed that complex 1 interacts with BSA more strongly than the other complexes. Yet again, complex 1 showed better activity due to the tridentate coordination of the ligand and cationic nature of the complex.<sup>43</sup>

Generally, quenching occurs through either dynamic or static quenching. The dynamic quenching is a process in which the

**Table 5. Quenching Constant ( $K_q$ ), Binding Constant ( $K_{bin}$ ), and Number of Binding Sites ( $n$ ) for the Interactions of Complexes with BSA**

complexes	$K_q$ ( $M^{-1}$ )	$K_{bin}$ ( $M^{-1}$ )	$n$
complex 1	$7.75(\pm 0.05) \times 10^4$	$1.69(\pm 0.03) \times 10^5$	1.29
complex 2	$5.99(\pm 0.02) \times 10^4$	$1.33(\pm 0.04) \times 10^4$	0.86
complex 3	$6.77(\pm 0.06) \times 10^4$	$1.54(\pm 0.04) \times 10^4$	1.08
complex 4	$6.48(\pm 0.86) \times 10^4$	$1.10(\pm 0.09) \times 10^5$	0.84

fluorophore and the quencher come into contact during the transient existence of the excited state, whereas static quenching refers to the formation of fluorophore–quencher complex in the ground state. The easiest method to determine the type of quenching is UV–visible absorption spectroscopy. Figure 10

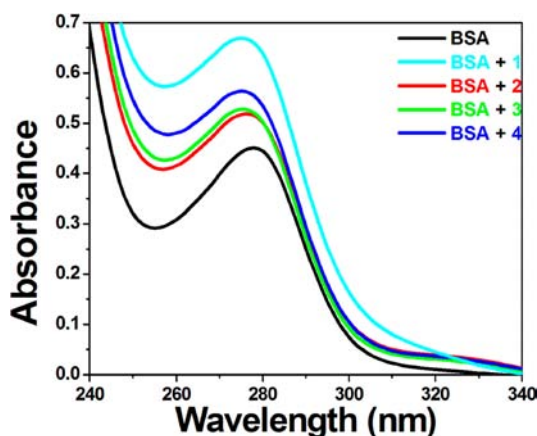


**Figure 10.** UV absorption spectra of BSA ( $10 \mu M$ ) in the presence of complexes 1 (A), 2 (B), 3 (C), and 4 (D) (0 and  $5 \mu M$ ).

shows the UV–visible spectra of BSA in the absence and presence of the complexes, which indicated that the absorption intensity of BSA was enhanced as the complexes were added, and there was a little blue shift of about 1 nm for all the complexes. It revealed the existence of a static interaction between BSA and the tested complexes.<sup>43</sup>

**Characteristics of Synchronous Fluorescence Spectra.** With an aim to investigate in detail the structural changes that occurred to BSA upon the addition of new complexes, synchronous fluorescence spectra of BSA were also measured before and after the addition of test compounds. Results from such studies usually provide reasonable information on the molecular microenvironment, particularly in the vicinity of the fluorophore functional groups.<sup>22</sup> Because of the presence of tyrosine, tryptophan, and phenylalanine residues, the BSA has fluorescence properties, and hence, spectroscopic methods are usually applied to study the conformation of serum protein. According to Miller,<sup>44</sup> the difference between the excitation wavelength and emission wavelength ( $\Delta\lambda = \lambda_{emi} - \lambda_{exc}$ ) indicates the types of chromophores. A higher  $\Delta\lambda$  value, such as 60 nm, is indicative of the characteristic of the tryptophan residue, whereas a lower  $\Delta\lambda$  value, such as 15 nm, is characteristic of the tyrosine residue.<sup>26</sup> Figures S5 and S6 (Supporting Information) depict the synchronous fluorescence spectra of BSA with various concentrations of test complexes recorded at  $\Delta\lambda = 15$  nm and  $\Delta\lambda = 60$  nm, respectively. In the synchronous fluorescence spectra of BSA at  $\Delta\lambda = 15$ , increasing the complexes to the solution of BSA resulted in an increase of the fluorescence intensity of BSA at 302 nm, 1.55, 1.32, 1.58,

and 1.51 times of the initial fluorescence intensity of BSA for complexes 1–4, respectively. However, in the case of synchronous fluorescence spectra of BSA at  $\Delta\lambda = 60$ , an increase in the concentration of the complexes to the solution of BSA resulted in a significant decrease of the fluorescence intensity of BSA at 344 nm, up to 65.55, 57.48, 60.97, and 63.98% of the initial fluorescence intensity of BSA accompanied by a trivial blue shift of 1 or 2 nm for complexes 1–4. The above spectral results indicated that the fluorescence intensities of the tryptophan were decreased with increasing concentration of the complexes. At the same time, there is no change in the emission wavelength of tyrosine. It suggested that the interaction of compounds with BSA affects the conformation of the tryptophan microregion.<sup>21</sup> It additionally points out that the hydrophobicity around tryptophan residues is strengthened. The hydrophobicity observed in fluorescence and synchronous measurements confirmed the effective binding of all the complexes with the BSA. Therefore, the observed interaction of these complexes with BSA suggested that the new palladium(II) complexes may be suitable for anticancer studies.

**Evaluation of Antioxidant Properties of the Complexes.** In addition to DNA and protein binding studies, we were interested in finding out the radical scavenging properties of the synthesized complexes. The antioxidative properties of 2-oxo-1,2-dihydroquinoline-3-carbaldehyde thiosemicarbazones and their metal complexes have attracted a lot of interests recently and have been extensively investigated, mainly in the in vitro systems.<sup>22,23</sup> The antioxidant potential of the new palladium complexes along with standards butylated hydroxyanisole (BHA) and butylated hydroxytoluene (BHT) in cell-free systems have been examined with reference to nitric oxide (NO), DPPH radicals (DPPH $\cdot$ ), hydroxyl radicals (OH $\cdot$ ), and superoxide anion radicals (O $_2^{\cdot-}$ ), and their corresponding IC $_{50}$  (determination of 50% activity) values are given in Table 6.

**Table 6. IC $_{50}$  Values (in  $\mu M$ ) Calculated from Various Radical Scavenging Assays of Complexes (1–4) and Standards (BHA and BHT)**

compound	NO	DPPH $\cdot$	OH $\cdot$	O $_2^{\cdot-}$
1	$18.3 \pm 1.5$	$7.21 \pm 0.52$	$10.3 \pm 1.2$	$25.1 \pm 3.8$
2	$39.7 \pm 2.2$	$19.3 \pm 2.7$	$27.3 \pm 2.3$	$42.4 \pm 3.9$
3	$30.8 \pm 3.3$	$18.7 \pm 1.5$	$25.8 \pm 1.4$	$43.1 \pm 1.5$
4	$21.2 \pm 1.7$	$10.2 \pm 0.4$	$22.1 \pm 1.9$	$28.3 \pm 1.4$
BHA	$629 \pm 12$	$9.81 \pm 0.55$	$317 \pm 8$	$295 \pm 9$
BHT	$723 \pm 8$	$9.12 \pm 0.73$	$272 \pm 9$	$287 \pm 8$

From the results obtained, it can be concluded that all the complexes possess potent free radical scavenging activity compared to the standard antioxidants in all the experiments. However, complexes 2–4 have less activity compared to standards in DPPH $\cdot$  scavenging activity. In the cases of NO, OH $\cdot$ , and O $_2^{\cdot-}$ , all the complexes showed very high activity than that of the standards, BHA and BHT, which is in the range of 10–50 times better. It is to be noted that complex 1 has good radical scavenging activity compared to the rest of the complexes, which may be due to the extended  $\pi$ -conjugation.

**In Vitro Cytotoxic Activity Evaluation of the Compounds.** The positive results obtained from the DNA binding, BSA binding, and antioxidative studies for the palladium(II) complexes 1–4 have stimulated us to test their ability to inhibit cell growth and induce cell death in the selected human cancer cell lines, human cervical cancer cells (HeLa), human skin

Table 7. Cytotoxic Activity of the Compounds

compound	IC <sub>50</sub> values ( $\mu\text{M}$ )				
	HeLa	A431	Hep G2	HEp-2	NIH 3T3
1	10.3 $\pm$ 0.9	20.1 $\pm$ 1.9	5.67 $\pm$ 0.45	24.3 $\pm$ 3.6	340 $\pm$ 11
2	27.7 $\pm$ 1.2	28.2 $\pm$ 1.5	17.1 $\pm$ 1.5	46.2 $\pm$ 2.3	295 $\pm$ 9
3	29.5 $\pm$ 1.7	25.4 $\pm$ 1.8	18.2 $\pm$ 1.2	31.3 $\pm$ 2.7	392 $\pm$ 15
4	15.1 $\pm$ 1.4	25.6 $\pm$ 1.2	11.3 $\pm$ 1.1	30.1 $\pm$ 3.9	385 $\pm$ 8
cisplatin	13.2 $\pm$ 0.8	15.6 $\pm$ 3.3	17.9 $\pm$ 2.1	16.8 $\pm$ 1.9	251 $\pm$ 12
H-Qtsc-H	389 $\pm$ 10	358 $\pm$ 9	395 $\pm$ 13	352 $\pm$ 10	389 $\pm$ 10
H-Qtsc-Me	375 $\pm$ 7	402 $\pm$ 10	386 $\pm$ 10	393 $\pm$ 12	301 $\pm$ 7
H-Qtsc-Et	399 $\pm$ 8	379 $\pm$ 9	369 $\pm$ 12	384 $\pm$ 11	322 $\pm$ 7
H-Qtsc-Ph	356 $\pm$ 8	376 $\pm$ 8	372 $\pm$ 9	375 $\pm$ 12	316 $\pm$ 10
[Pd(PPh <sub>3</sub> ) <sub>2</sub> Cl <sub>2</sub> ]	299 $\pm$ 5	288 $\pm$ 10	287 $\pm$ 9	283 $\pm$ 8	219 $\pm$ 9

cancer cells (A431), human liver carcinoma cells (Hep G2), and human laryngeal epithelial carcinoma cells (HEp-2). Complexes were dissolved in DMSO, and blank samples containing same volume of DMSO were taken as controls to identify the activity of solvent in the cytotoxicity experiment. The IC<sub>50</sub> values obtained for the free ligands, metal precursors, and the new complexes against the cell lines are listed in Table 7. It is to be noted that the ligands and the Pd(II) metal precursors did not show any significant activity on all the cells under our experimental conditions, which confirmed that the chelation of the ligand with the Pd(II) ion is the only responsible factor for the observed cytotoxic properties of the new complexes. The results indicate that all of the palladium complexes exhibited antitumor activities against the human cancer cell lines. Moreover, they exhibited better cytotoxicity against the Hep G2 cancer cell line than the other three cancer cells, which clearly indicates that our complexes are more specific on a particular cancer cell (Hep G2). Interestingly, on comparison of the IC<sub>50</sub> value of complex 1 with cisplatin against Hep G2, the inhibitory activity of 1 against Hep G2 is about 3 times higher than that of cisplatin. From the above results, we observed that complex 1 showed better activity when compared to the rest of the complexes, which may be due to an increase in chelation of the ligand with the Pd(II) ion, cationic nature, and enhanced planarity of the complex. In addition, the *in vitro* cytotoxic activity studies of the new complexes against NIH 3T3 mouse embryonic fibroblasts (normal cells) and the IC<sub>50</sub> value of the complexes have been found to be above 300  $\mu\text{M}$ , which confirmed that the complexes are very specific on cancer cells. Moreover, when we compare these observations with our earlier results of Cu(II) thiosemicarbazone complexes, it is inferred that these Pd(II) complexes have higher cytotoxic potentials than that of the Cu(II) complexes.<sup>22</sup>

## CONCLUSION

A series of new palladium(II) complexes of 2-oxo-1,2-dihydroquinoline-3-carbaldehyde 4*N*-substituted thiosemicarbazones have been prepared and characterized by various spectral techniques. The molecular structures of complexes 1–4 have been confirmed by single-crystal X-ray diffraction studies, which revealed that, whereas the unsubstituted thiosemicarbazone ligand coordinates to palladium in a monobasic tridentate (ONS<sup>-</sup>) manner via the oxo oxygen, imine nitrogen, and thiolate sulfur, the other three ligands coordinated in a monobasic bidentate (NS<sup>-</sup>) manner via the imine nitrogen and thiolate sulfur. The DNA binding results showed that all the complexes bind with DNA via intercalation. In addition, the protein interaction properties of the new

complexes were studied by UV–visible and fluorescence spectroscopies, and the results indicated that the cationic nature of complex 1 has resulted in strong binding compared with the rest of the complexes. The new palladium(II) complexes have been tested for their free radical scavenging activity. Moreover, all the new complexes were screened for antitumor activity against HeLa, A431, Hep G2, and HEp-2 cancer cell lines, and they were found to exhibit excellent cytotoxicity to cancer cell without affecting the normal NIH 3T3 cells. In all the above experimental results, we observed that complex 1 has the most significant activity, which may be due to the cationic nature of the complex and the presence of tridentate chelation of the ligand.

## ASSOCIATED CONTENT

### Supporting Information

Pseudo binuclear structure of complexes 1–4 (Figures S1–S4) and synchronous spectra of BSA (1  $\mu\text{M}$ ) in the presence of increasing amounts of complexes 1 (A), 2 (B), 3 (C), and 4 (D) (0–25  $\mu\text{M}$ ) in the wavelength difference of  $\Delta\lambda = 15$  nm and  $\Delta\lambda = 60$  nm (Figures S5 and S6). This material is available free of charge via the Internet at <http://pubs.acs.org>. Crystallographic data for the structures reported in this paper have been deposited with the Cambridge Crystallographic Data Centre (CCDC) as supplementary publication numbers CCDC-905160, 905161, 905162, and 905163 for the palladium complexes 1–4. Copies of the data can be obtained free of charge from the CCDC (12 Union Road, Cambridge CB2 1EZ, U.K.; Tel: +44–1223–336408; Fax: +44–1223–336003; E-mail: [deposit@ccdc.cam.ac.uk](mailto:deposit@ccdc.cam.ac.uk); Web site: <http://www.ccdc.cam.ac.uk>).

## AUTHOR INFORMATION

### Corresponding Author

\*Tel: +91 422 2428319. Fax: +91 422 2422387. E-mail: [k\\_natraj6@yahoo.com](mailto:k_natraj6@yahoo.com).

### Notes

The authors declare no competing financial interest.

## ACKNOWLEDGMENTS

Council of Scientific and Industrial Research (CSIR), New Delhi, India [Grant No. 21(0745)/09/EMR-II] is gratefully acknowledged for the financial assistance and for the award of SRF to E.R.

## REFERENCES

- (1) Kostova, I. *Recent Pat. Anti-Cancer Drug Discovery* 2006, 1, 1–22.

- (2) Boulikas, T.; Vougiouka, M. *Oncol. Rep.* **2003**, *10*, 1663–1682.
- (3) Wong, E.; Giandomenico, C. M. *Chem. Rev.* **1999**, *99*, 2451–2466.
- (4) Galanski, M.; Arion, V. B.; Jakupec, M. A.; Keppler, B. K. *Curr. Pharm. Des.* **2003**, *9*, 2078–2089.
- (5) Wang, D.; Lippard, S. J. *Nat. Rev. Drug Discovery* **2005**, *4*, 307–320.
- (6) Ruiz, J.; Cutillas, N.; Vicente, C.; Villa, M. D.; Lopez, G. *Inorg. Chem.* **2005**, *44*, 7365–7376.
- (7) Gao, E. J.; Liu, C.; Zhu, M. C.; Lin, H. K.; Wu, Q.; Liu, L. *Anti-Cancer Agents Med. Chem.* **2009**, *9*, 356–368.
- (8) Daghriri, H.; Huq, F.; Beale, P. *Coord. Chem. Rev.* **2004**, *248*, 119–133.
- (9) Gao, E.; Liu, C.; Zhu, M.; Lin, H.; Wu, Q.; Liu, L. *Anti-Cancer Agents Med. Chem.* **2009**, *9*, 356–368.
- (10) Abu-Surrah, A. S.; Kettunen, M. *Curr. Med. Chem.* **2006**, *13*, 1337–1357.
- (11) Caires, A. C. F. *Anti-Cancer Agents Med. Chem.* **2007**, *7*, 484–491.
- (12) Abu-Surrah, A. S.; Al-Sadoni, H. H.; Abdalla, M. Y. *Cancer Ther.* **2008**, *6*, 1–10.
- (13) Souza, P.; Matesanz, A. I. In *Palladium: Compounds, Production and Applications*; Brady, K.M., Ed.; Nova Science Publishers: New York, 2011.
- (14) Matesanz, A. I.; Hernandez, C.; Rodriguez, A.; Souza, P. J. *Inorg. Biochem.* **2011**, *105*, 1613–1622.
- (15) Nordell, P.; Lincoln, P. J. *Am. Chem. Soc.* **2005**, *127*, 9670–9671.
- (16) Barraja, P.; Diana, P.; Montalbano, A.; Dattolo, G.; Cirrincione, G.; Viola, G.; Vedaldi, D.; Acqua, F. D. *Bioorg. Med. Chem.* **2006**, *14*, 8712–8728.
- (17) Kuethe, J. T.; Wong, A.; Qu, C. X.; Smithtrovich, J.; Davies, I. W.; Hughes, D. L. *J. Org. Chem.* **2005**, *70*, 2555–2567.
- (18) Prabhakaran, R.; Kalaivani, P.; Jayakumar, R.; Zeller, M.; Hunter, A. D.; Renukadevi, S. V.; Ramachandran, E.; Natarajan, K. *Metallomics* **2011**, *3*, 42–48.
- (19) Kalaivani, P.; Prabhakaran, R.; Dallemer, F.; Poornima, P.; Vaishnavi, E.; Ramachandran, E.; Vijaya Padma, V.; Renganathan, R.; Natarajan, K. *Metallomics* **2012**, *4*, 101–113.
- (20) Ramachandran, E.; Kalaivani, P.; Prabhakaran, R.; Rath, N. P.; Brinda, S.; Poornima, P.; Vijaya Padma, V.; Natarajan, K. *Metallomics* **2012**, *4*, 218–227.
- (21) Kalaivani, P.; Prabhakaran, R.; Ramachandran, E.; Dallemer, F.; Paramaguru, G.; Renganathan, R.; Poornima, P.; Vijaya Padma, V.; Natarajan, K. *Dalton Trans.* **2012**, *41*, 2486–2499.
- (22) Senthil Raja, D.; Paramaguru, G.; Bhuvanesh, N. S. P.; Reibenspies, J. H.; Renganathan, R.; Natarajan, K. *Dalton Trans.* **2011**, *40*, 4548–4559.
- (23) Senthil Raja, D.; Bhuvanesh, N. S. P.; Natarajan, K. *Eur. J. Med. Chem.* **2011**, *46*, 4584–4594.
- (24) Ramachandran, E.; Kalaivani, P.; Prabhakaran, R.; Zeller, M.; Bartlett, J. H.; Adero, P. O.; Wagner, T. R.; Natarajan, K. *Inorg. Chim. Acta* **2012**, *385*, 94–99.
- (25) Ramachandran, E.; Thomas, S. P.; Poornima, P.; Kalaivani, P.; Prabhakaran, R.; Vijaya Padma, V.; Natarajan, K. *Eur. J. Med. Chem.* **2012**, *50*, 405–415.
- (26) Ramachandran, E.; Senthil Raja, D.; Bhuvanesh, N. S. P.; Natarajan, K. *Dalton Trans.* **2012**, *41*, 13308–13323.
- (27) Ramachandran, E.; Senthil Raja, D.; Bhuvanesh, N. S. P.; Natarajan, K. *RSC Adv.* **2012**, *2*, 8515–8525.
- (28) Vogel, A. I. *Text Book of Practical Organic Chemistry*, 5th ed.; Longman: London, 1989.
- (29) Burmeester, J. L.; Basolo, F. *Inorg. Chem.* **1964**, *3*, 1587–1593.
- (30) *Apex II and SAINT*; Bruker Analytical X-Ray: Madison, WI, 2008.
- (31) Sheldrick, G. M. *Acta Crystallogr.* **2008**, *A64*, 112–122.
- (32) Nash, T. *Biochem. J.* **1953**, *55*, 416–421.
- (33) Klein, S. M.; Cohen, G.; Cederbaum, A. I. *Biochemistry* **1981**, *20*, 6006–6012.
- (34) Green, L. C.; Wagner, D. A.; Glogowski, J.; Skipper, P. L.; Wishnok, J. S.; Tannenbaum, S. R. *Anal. Biochem.* **1982**, *126*, 131–138.
- (35) Blois, M. S. *Nature* **1958**, *29*, 1199–1200.
- (36) Beauchamp, C.; Fridovich, I. *Anal. Biochem.* **1971**, *44*, 276–287.
- (37) Blagosklonny, M.; El-diery, W. S. *Int. J. Cancer* **1996**, *67*, 386–392.
- (38) Krishnamoorthy, P.; Sathyadevi, P.; Cowley, A. H.; Butorac, R. R.; Dharmaraj, N. *Eur. J. Med. Chem.* **2011**, *46*, 3376–3387.
- (39) Senthil Raja, D.; Bhuvanesh, N. S. P.; Natarajan, K. *Eur. J. Med. Chem.* **2012**, *47*, 73–85.
- (40) Wolf, A.; Shimer, G. H.; Meehan, T. *Biochemistry* **1987**, *26*, 6392–6396.
- (41) Meyer-Almes, F. J.; Porschke, D. *Biochemistry* **1993**, *32*, 4246–4253.
- (42) Howe, G. M.; Wu, K. C.; Bauer, W. R. *Biochemistry* **1976**, *19*, 339–347.
- (43) Senthil Raja, D.; Bhuvanesh, N. S. P.; Natarajan, K. *Inorg. Chem.* **2011**, *50*, 12852–12866.
- (44) Miller, J. N. *Proc. Anal. Div. Chem. Soc.* **1979**, *16*, 203–208.